

INFALL CAUSTICS IN DARK MATTER HALOS?

JÜRG DIEMAND^{1,2} AND MICHAEL KUHLEN³*Draft version April 25, 2008*

ABSTRACT

We show that most particle and subhalo orbits in simulated cosmological cold dark matter halos are surprisingly regular and periodic: The phase space structure of the outer halo regions shares some of the properties of the classical self-similar secondary infall model. Some of the outer branches are clearly visible in the radial velocity - radius plane at certain epochs. However, they are severely broadened in realistic, triaxial halos with non-radial, clumpy, mass accretion. This prevents the formation of high density caustics: Even in the best cases there are only broad, very small ($< 10\%$) enhancements in the spherical density profile. Larger fluctuations in $\rho(r)$ caused by massive satellites are common. Infall caustics are therefore too weak to affect lensing or dark matter annihilation experiments. Their detection is extremely challenging, as it requires a large number of accurate tracer positions and radial velocities in the outer halo. The stellar halo of the Milky Way is probably the only target where this could become feasible in the future.

Subject headings: dark matter — galaxies: formation – Galaxy: halo – methods: n-body simulations

1. INTRODUCTION

Idealized models of self-similar, radial infall onto an initial spherical overdensity in an expanding and otherwise homogenous universe can be solved exactly (Fillmore & Goldreich 1984; Bertschinger 1985) (FGB hereafter). The two key predictions of these models are: (i) Nearly isothermal ($\rho \propto r^{-2}$) halo density profiles, as found in earlier models (Gott 1975; Gunn 1977). (ii) Near their apocenters mass shells pile up and form spherical caustic surfaces of infinite density. This occurs at constant fractions of the *current* turnaround radius, resulting in slowly outward moving caustics as the turnaround radius increases with time. Each mass shell moves on a radial orbit with a nearly fixed (only slowly decreasing) apocenter of about 0.85 of *its own* turnaround radius. After a shell falls in it forms part of the first (outermost) caustic when the shell is near its first apocenter passage. Later, near its second apocenter, it forms part of the second caustic, and so on. Such caustics would increase the dark matter annihilation rate (Bergström et al. 2001; Mohayaee & Shandarin 2006), and it has been argued that infall would lead to peaks in the local CDM velocity distribution and change the predictions for direct dark matter detection (Sikivie et al. 1997).

Both key predictions of the original FGB-model are at odds with the properties of dark matter halos found in cosmological simulations: Halo density profiles are found to be steeper than $\rho \propto r^{-2}$ in the outer parts and shallower in the inner regions (Dubinski & Carlberg 1991; Navarro et al. 1996). However, by relaxing some of the simplifying assumptions of the FGB-model it is possible to obtain a more realistic secondary infall model which successfully reproduces the halo density profiles found in cosmological simulations (e.g. Ascasibar et al. 2007 and references therein): allowing for angular momen-

tum lowers the inner densities relative to the original $\rho \propto r^{-2.25}$ profile, simply because fewer particles orbit through the central regions (Ryden 1993). More realistic initial perturbations lead to a steeper outer profile (Hoffman & Shaham 1985).

Infall does not lead to high density caustic surfaces in cosmological simulations. In early simulations most particle orbits differed widely from the slowly shrinking, nearly periodic orbits found in the FGB-model (Zaroubi et al. 1996). But these simulations contained only a few thousand particles, which leads to significantly distorted orbits due to artificial two body relaxation (Diemand et al. 2004b). Despite the numerical noise, Zaroubi et al. (1996) found that the final particle energies are strongly correlated with the initial ones, suggesting a rather gentle, orderly halo build-up as in FGB, and not violent relaxation. Another consequence of this fairly regular build-up is that material from biased, early high density regions ends up in the inner parts of halos today (Diemand et al. 2005). However, recent high resolution simulations still produce rather smooth mass profiles without high density caustics (e.g. Moore et al. 2001; Helmi et al. 2002; Diemand et al. 2007). Moore (2001) emphasized that in the hierarchical buildup of CDM halos the internal velocity dispersion of infalling satellites σ_{sat} is typically only a few times smaller than σ_{host} , which would broaden caustics significantly, to a width of about $R_{\text{host}}\sigma_{\text{sat}}/\sigma_{\text{host}}$. Indeed resolved mergers do bring in practically all the mass and there is no evidence for smooth accretion (Madau et al. 2008). Here we show that despite clumpy, non-radial, anisotropic accretion into a non-spherical potential, the outer parts of halos do show a few weak, broad branches in $v_r - r$ -space. Their properties agree well with some of the FGB predictions. In contrast to the model however, realistic infall "caustics"⁴ increase the dark matter densities only slightly ($\simeq 10\%$ for the strongest ones). Unfortunately

¹ University of California, High Street 1156, Santa Cruz, CA 95064; diemand@ucolick.org

² Hubble Fellow

³ Institute for Advanced Study, Einstein Drive, Princeton, NJ 0854; mqk@ias.edu

⁴ For brevity we refer to the turnaround regions of branches in $v_r - r$ -space simply as "caustics", even though they don't have the high densities implied by the true sense of the word.

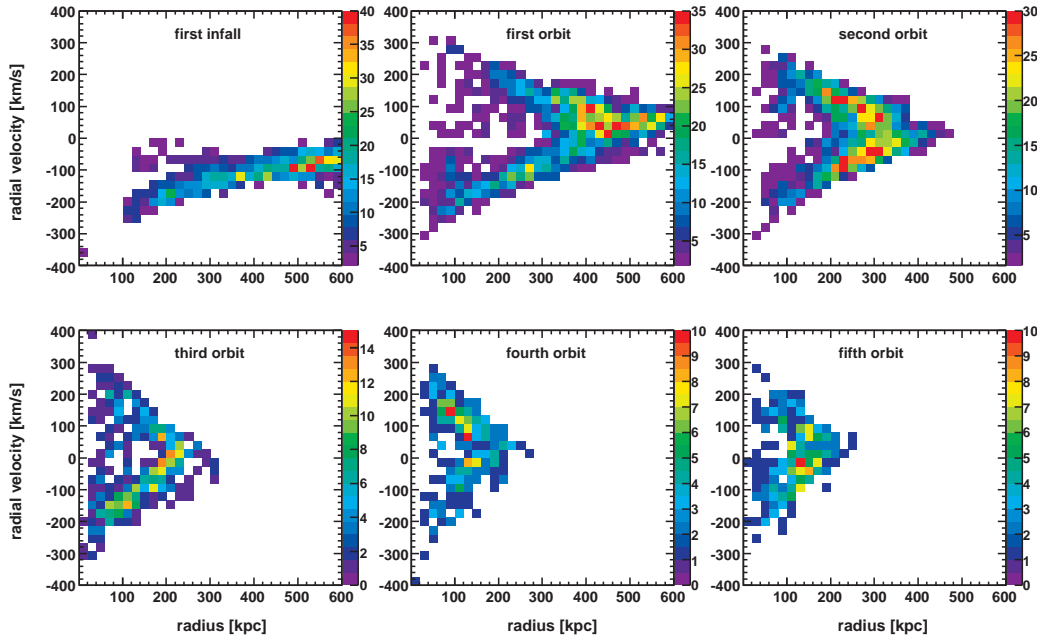


FIG. 1.— Phase space distribution of subhalos at $z=0$ separated by the number of orbits they have completed. This figure is also available as an mpeg animation running from $z=12$ to 0 in the electronic edition of ApJ.

this makes them practically undetectable and irrelevant for dark matter detection.

2. WEAK OUTER CAUSTICS IN $V_R - R$ SPACE

In this section we compare the histories of subhalos in the Via Lactea simulation (Diemand et al. 2007, VL07 hereafter)⁵ with predictions from the FGB-model. Later we will include the distribution of all dark matter particles. The subhalos are selected by peak circular velocity $V_{\max} > 3 \text{ km s}^{-1}$ *before* accretion, and are therefore very similar to dark matter particles in their spatial and velocity distribution (Faltenbacher & Diemand 2006). This sample contains 10,652 halos and subhalos with masses above about $3 \times 10^6 M_\odot$. The host halo has size of $V_{\max} = 181 \text{ km s}^{-1}$, consistent with the dark halo of the Milky Way. The subhalos which have completed the same small number of orbits end up in a relatively narrow branch in $v_r - r$ space, despite their range of orbital eccentricities (VL07), the prolate host halo potential (about 0.8:1, see Kuhlen et al. 2007) and occasional kicks from larger satellites (Sales et al. 2007). Each panel in Figure 1 would correspond to one infinitesimally thin branch in the $v_r - r$ plane of the FGB-model. Already at first infall the radial and tangential velocity dispersions are quite large: $\sigma_r \simeq 26 \text{ km s}^{-1}$ and $\sigma_{\text{tan},2D} \simeq 60 \text{ km s}^{-1}$. These motions induced by large scale tidal forces and also by structures forming within the turnaround region prevent the formation of thin, high density caustics.

From the positions of subhalos near their apocenter we can measure the position and width of the outer six infall caustics (Table 1). In the FGB-model the radial velocity of a caustic at radius r is $v_{\text{caustic}}(r) = 8/9 r/t$, where t is the time since the Big Bang⁶. We define those sub-

halos near their k^{th} apocenter passage and with a radial velocity within 24 km s^{-1} of $v_{\text{caustic}}(r)$ as the members of caustic k . For each member i we then determine its turnaround radius $t_{k,i}$ and the ratio of today's position to turnaround radius $r_{k,i}/t_{k,i}$. Note that members of one caustic fell in from all directions, not as a bound group, and merely share similar turnaround times and radii. The scatter in the turnaround radii is relatively large and comparable to the width of the caustics. This again hints at a broadening of caustics caused already early (near the turnaround time) by proper motions. Caustics 4, 5, and 6 are so wide that they completely overlap, and they disappear in the full $v_r - r$ plot of all particles (Figure 2). Caustic 3 is the most prominent one at $z=0$ and it leads to a small over-density of about 10% over a smooth density profile around 220 kpc. The abundance of particles with $|v_r - v_{\text{caustic}}| < 24 \text{ km s}^{-1}$ increases by a factor of about 1.6 around 220 kpc. The outermost caustics 1 and 2 are quite wide, but parts of their corresponding branches from Figure 1 are still visible in Figure 2. Note that all of the outer three $v_r - r$ branches have large gaps, which are caused by epochs of little or no mass accretion. The animated versions of Figures 1 and 2 shows how these phase-space features and the gaps in between form and move. Whether a certain branch is currently visible in the $v_r - r$ plane depends on whether there was enough mass falling in at some earlier time to reach a sufficient density in the corresponding region of phase-space. The clearest caustic at $z=0$ is the third one; it was generated by continuous, large infall of material around $z=1.7$. At later epochs Via Lactea's mass accretion becomes quite small and sporadic (VL07), leading to weak first and second branches with large gaps. The Via Lactea halo formed in a series of major mergers before $z=1.7$. These mergers could be responsible for a broad-

⁵ Subhalo histories, animated versions of Figures 1 and 2 and other movies are available at www.uchicago.edu/~diemand/vl

⁶ For simplicity we assume this formula derived by FGB in an

$\Omega_m = 1$ universe to be approximately right also in Λ CDM.

TABLE 1
POSITIONS AND WIDTHS OF CAUSTICS AND TURNAROUND REGIONS IN THE VIA LACTEA HALO.

k	$r_{k,\text{med}}$ [kpc]	$r_{k,68\%}$ [kpc]	$\frac{\Delta r_k}{r_{k,\text{med}}}$	$t_{k,\text{med}}$ [kpc]	$t_{k,68\%}$ [kpc]	$\frac{\Delta t_k}{t_{k,\text{med}}}$	$\left(\frac{r_k}{t_k}\right)_{\text{med}}$	$\left(\frac{r_k}{t_k}\right)_{68\%}$	$\left(\frac{r_k}{t_k}\right)_{\text{FGB}}$	$\frac{r_{k,\text{med}}}{r_{1,\text{med}}}$	$\left(\frac{r_k}{r_1}\right)_{\text{FGB}}$
1	453	370–534	0.36	491	443–551	0.22	0.92	0.77–1.12	0.876	1	1
2	310	242–384	0.46	343	297–407	0.32	0.93	0.57–1.24	0.864	0.68	0.65
3	220	204–237	0.15	261	211–316	0.40	0.84	0.67–1.10	0.856	0.49	0.49
4	173	137–207	0.41	222	180–266	0.39	0.78	0.58–1.25	0.843	0.38	0.40
5	141	110–191	0.57	179	131–229	0.55	0.78	0.52–1.46	0.832	0.31	0.34
6	121	89–170	0.67	157	105–201	0.61	0.81	0.54–1.46	0.834	0.27	0.30

NOTE. — Positions and widths of the outer six caustics r_k and turnaround radii of the particles in the caustic t_k . Median values and 68% ranges of all caustic members are given, Δ refers to the full width of the 68% range. The number of subhalo members in the caustics 1 to 6 are 551, 300, 49, 32, 56 and 15. "FGB" refers to predictions from the secondary infall model.

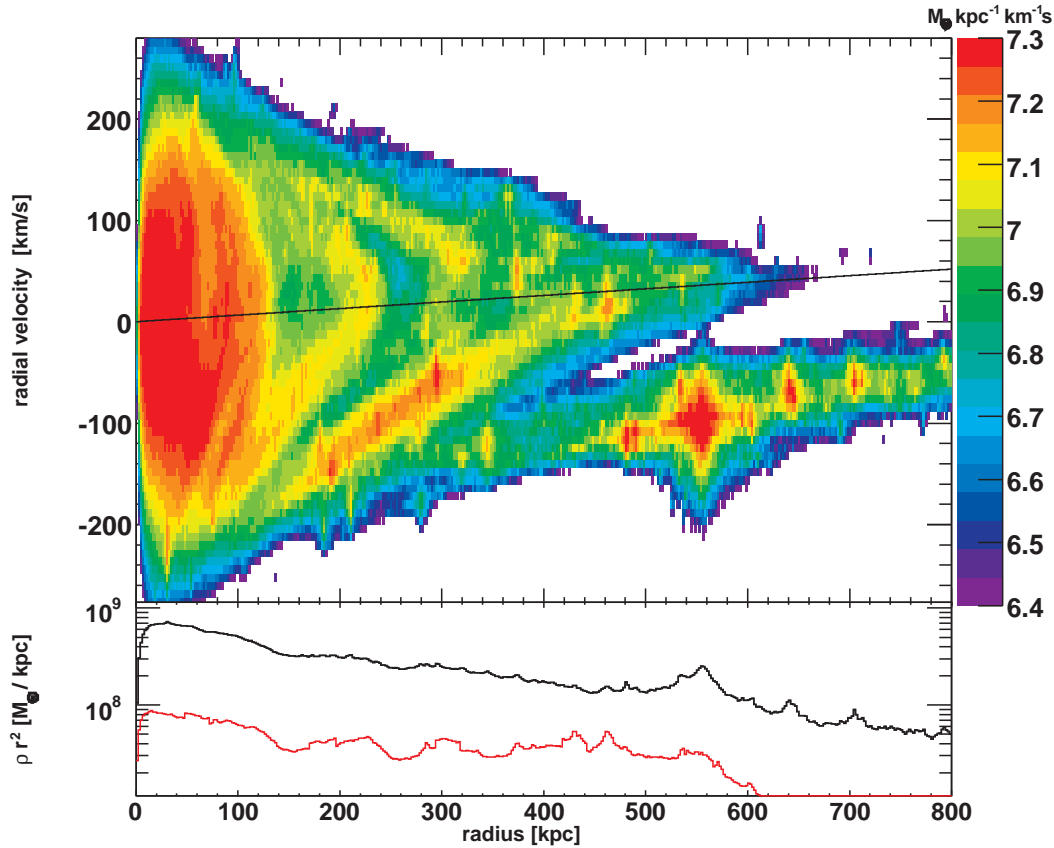


FIG. 2.— Phase space distribution of the dark matter particles at $z=0$. The straight line is $v_{\text{caustic}}(r)$. The lower panel shows the $\rho(r)r^2$ of all particles (black) and of a subset with $|v_r - v_{\text{caustic}}| < 24 \text{ km s}^{-1}$ (red). This figure is also available as an mpeg animation running from $z=12$ to 0 in the electronic edition of ApJ.

ening of the fourth and higher caustics to a degree where they become completely washed out and undetectable in the $z=0$ snapshot.

3. COMPARISON WITH THE FGB-MODEL

In Table 1 we make some quantitative comparisons with the $\epsilon = 1$ version of the FGB-model, which corresponds to a point-mass as initial over-density: $\delta = \delta M/M \propto M^{-\epsilon}$. In CDM the initial peaks are extended. The Via Lactea halo has $\epsilon \simeq 0.2$ up to about $10^{11} M_{\odot}$. For larger masses ϵ increases and it is about one at $10^{12} M_{\odot}$, equivalent to a scale of 150 kpc today. The outer halo features discussed here correspond to the $\epsilon \simeq 1$

regime⁷.

The FGB-model was solved for an Einstein-de Sitter ($\Omega_m = 1$) universe, while the Via Lactea simulation assumed the now standard Λ CDM model, but we do not believe that this difference affects our results: In the model, the position of a caustic is similar (0.8 to 0.9) to the turnaround radius of the caustic members. Members of the first caustic turned around before $z=1$ (earlier for higher caustics), when the Λ CDM model was still matter dominated and similar to an Einstein-de Sitter universe.

⁷ Larger collapse factors in the inner halo (see Fig. 1 in VL07) might be related to the smaller r_k/t_k ratios in the $\epsilon = 0.2$ FGB-model.

After turnaround the enclosed mass dominates over the enclosed vacuum energy and the dynamics are practically the same in both cosmologies.

We find that the ratios of the current caustic positions are in good agreement with the FGB-model (Table 1). Also the median of the ratios of caustic radii to turnaround radii $(r_k/t_k)_{\text{med}}$ agree quite well with the FGB-model, i.e. the typical orbits go out close to their turnaround scale. Earlier models (Gunn 1977) assumed they would decrease by a factor of two during virialization. This assumption is also made in the definition of the formal virial radius⁸, which therefore only encloses a fraction of the material orbiting around a galaxy (Prada et al. 2006, VL07). The $(r_k/t_k)_{\text{med}}$ in the clusters from (Diemand et al. 2004a) are also close to 0.85, i.e. the orbits of bound material extend well beyond the formal virial radius both in galaxy and cluster halos⁹.

The main difference between the FGB-model and cosmological halos is the large scatter in space and velocity around the lines in $v_r - r$ space on which all matter is found in the model. The scatter prevents the formation of high density caustic surfaces and makes the broad caustic-like features from cosmological infall practically undetectable: To find them one needs an accurate, large sample of $v_r - r$ measurements, which are available in simulations, but unfortunately not in the real Universe. For members of the outer four caustics the scatter in the individual r_k/t_k ratios is consistent with the shape of the potential in the outer parts of Via Lactea halo, which is about 1:0.8 prolate at $z=0$ and about 1:0.7 prolate at $z=0.5$ (Kuhlen et al. 2007). We also find a few outliers with much larger r_k/t_k ratios, probably resulting from dynamical interactions between multiple satellites (Sales et al. 2007). The scatter is significantly larger for the 5th and 6th caustics, presumably because this material was accreted early ($z > 1.7$), when a series of major mergers caused large fluctuations in the host potential.

4. MULTIMODAL RADIAL VELOCITY DISTRIBUTIONS

From Figure 2 it is clear that the radial velocity distribution of particles in a shell in the outer halo will not be smooth and unimodal, but rather a superposition of modes caused by the various branches in $v_r - r$ space. The velocity distribution and relative importance of each mode changes with distance from the galactic center, and fewer modes are present at large radii (Figure 3).

The subhalo radial velocity distributions are similar to those of particles and we can use subhalo histories to illustrate how the particle distributions divide up into their components. Between caustics 2 and 3 one finds a broad, doubly peaked distribution. The negative velocity peak is a superposition of first infall and subhalos approaching the center on the second half of their first or second orbit. The subhalos on first infall have the most negative typical velocities, followed by those on their first and second orbit, in qualitative agreement with the FGB-model. In contrast to the model, we find these components have wide radial velocity distributions which largely overlap and give rise to only one broad infalling

⁸ The virial radius of the Via Lactea halo is $r_{\text{vir}} = r_{104} = 288$ kpc. It encloses a mass of $M_{\text{vir}} = 1.5 \times 10^{12} M_{\odot}$.

⁹ Unlike galaxies halos, typical cluster halos do accrete a lot of mass around $z = 0$ leading to a net infall between their formal virial radius and the turnaround radius (Cuesta et al. 2007).

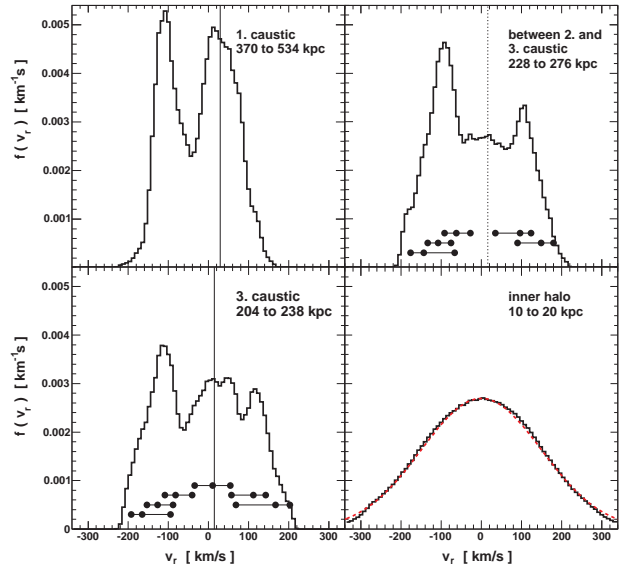


FIG. 3.— Radial velocity distributions of particles in different radial shells (solid lines). Only in the inner halo (lower right panel) the distribution is uni-modal and close to a Gaussian (dashed line). The other panels show multi-modal distributions. To illustrate how to decompose these particle distributions we also plot the median and 68% ranges of ingoing and outgoing subhalos, which have completed 0, 1 or 2 two orbits from bottom to top (circles). On the third caustic (lower left panel) the subhalos which have completed 3 orbits are now near their apocenter. The vertical lines give the local caustic velocity $v_{\text{caustic}}(r) = 8/9 r/t$.

peak. On the third caustic the broad, double peaked distribution from in- and outgoing material is the same as above, but now there is an additional peak at low radial velocity from particles near their third apocenter.

In the inner halo particles which completed the same number of orbits are distributed so widely that the total radial velocity distribution becomes one featureless peak. It is close to a Gaussian distribution with zero mean velocity and a dispersion of 150 km s^{-1} . But note that a smooth, inner $f(r, v_r)$ does not preclude the existence of coherent structures in the full phase-space density $f(\vec{x}, \vec{v})$, such as bound clumps (subhalos) and their unbound debris (tidal streams) (Moore et al. 2001; Helmi et al. 2002).

5. SUMMARY

We have discovered broad, caustic-like features in $f(r, v_r)$ in the outer parts of CDM halos from cosmological simulations. They are too broad to cause significant density enhancements and would therefore be very challenging to detect. Since a large number of accurate distances radial velocities are needed, we believe that the stellar halo of the Milky Way is the only system where one might possibly detect such features in the foreseeable future.

The basic properties of infall caustics are independent of redshift and halo mass; they are similar in the Via Lactea galaxy halo and in the cluster halos from Diemand et al. (2004a). The galaxy halos in that work were resolved with only a few million particles per halo and clearly show similar features. A new, one billion particle galaxy halo (Diemand et al. in prep.) also only shows broad, weak outer caustics. Since the features described here do not change qualitatively when the nu-

merical resolution is increased by almost three orders of magnitude we conclude that they are well resolved in simulations with a few million particles per halo.

We thank Ed Bertschinger and Roya Mohayaee for helpful discussions and Peter Goldreich, Roya Mohayaee

and Scott Tremaine for helpful comments on an earlier version of this letter. We acknowledge support from NASA through a Hubble Fellowship grant (JD) and from the Hansmann Fellowship at the Institute for Advanced Study (MK).

REFERENCES

- Ascasibar, Y., Hoffman, Y., & Gottlöber, S. 2007, *MNRAS*, 376, 393
- Bergström, L., Edsjö, J., & Gunnarsson, C. 2001, *Phys. Rev. D*, 63, 083515
- Bertschinger, E. 1985, *ApJS*, 58, 39
- Cuesta, A. J., Prada, F., Klypin, A., & Moles, M. 2007, *ArXiv e-prints*, 710
- Diemand, J., Kuhlen, M., & Madau, P. 2007, *ApJ*, 667, 859
- Diemand, J., Madau, P., & Moore, B. 2005, *MNRAS*, 364, 367
- Diemand, J., Moore, B., & Stadel, J. 2004a, *MNRAS*, 352, 535
- Diemand, J., Moore, B., Stadel, J., & Kazantzidis, S. 2004b, *MNRAS*, 348, 977
- Dubinski, J. & Carlberg, R. G. 1991, *ApJ*, 378, 496
- Faltenbacher, A. & Diemand, J. 2006, *MNRAS*, 369, 1698
- Fillmore, J. A. & Goldreich, P. 1984, *ApJ*, 281, 1
- Gott, J. R. I. 1975, *ApJ*, 201, 296
- Gunn, J. E. 1977, *ApJ*, 218, 592
- Helmi, A., White, S. D., & Springel, V. 2002, *Phys. Rev. D*, 66, 063502
- Hoffman, Y. & Shaham, J. 1985, *ApJ*, 297, 16
- Kuhlen, M., Diemand, J., & Madau, P. 2007, *ApJ*, 671, 1135
- Madau, P., Diemand, J., & Kuhlen, M. 2008, *ArXiv e-prints*, 802
- Mohayaee, R. & Shandarin, S. F. 2006, *MNRAS*, 366, 1217
- Moore, B. 2001, in *Identification of Dark Matter*, ed. N. J. C. Spooner & V. Kudryavtsev, 93–+
- Moore, B., Calcáneo-Roldán, C., Stadel, J., Quinn, T., Lake, G., Ghigna, S., & Governato, F. 2001, *Phys. Rev. D*, 64, 063508
- Navarro, J. F., Frenk, C. S., & White, S. D. M. 1996, *ApJ*, 462, 563
- Prada, F., Klypin, A. A., Simonneau, E., Betancort-Rijo, J., Patiri, S., Gottlöber, S., & Sanchez-Conde, M. A. 2006, *ApJ*, 645, 1001
- Ryden, B. S. 1993, *ApJ*, 418, 4
- Sales, L. V., Navarro, J. F., Abadi, M. G., & Steinmetz, M. 2007, *MNRAS*, 379, 1475
- Sikivie, P., Tkachev, I. I., & Wang, Y. 1997, *Phys. Rev. D*, 56, 1863
- Zaroubi, S., Naim, A., & Hoffman, Y. 1996, *ApJ*, 457, 50